# Magnetic core field anomalies in the non-axial field : approach with a monopole

Pablo Rivera[1,2], F. Javier Pavón-Carrasco[1,2], Angelo De Santis[3], M.L. Osete[1,2], Saioa A. Campuzano[1,2], Gianfranco Cianchini[3]

*1. Departamento de Física de la Tierra y Astrofísica, Universidad Complutense de Madrid (UCM), Plaza Ciencias, 1, Madrid – 28040 (Spain).*
*2. Instituto de Geociencias (IGEO, CSIC-UCM), C/ Doctor Severo Ochoa, 7, Madrid – 28040 (Spain).*
*3. Istituto Nazionale di Geofisica e Vulcanologia (INGV), Sezione Roma 2, Via di Vigna Murata 605, 00143 Rome, Italy.*

This presentation participates in OSPP
Outstanding Student & PhD candidate Presentation contest

## 1-INTRODUCTION

Global paleo-reconstructions are an essential tool for understanding the millennial past variations of the geomagnetic field at the surface and at the core-mantle boundary (CMB).

Within the Holocene epoch, two anomalies have become notably well-defined:

- **The South Atlantic Anomaly (SAA),** characterized by low geomagnetic intensities in the South Atlantic region almost during the last millennium, stands out as the most significant present-day anomaly.
- **The Levantine Iron Age Anomaly (LIAA)** defined as a geomagnetic spike characterized by abnormally high intensities affecting Levant and Europe during the first half of the first millennium BCE.

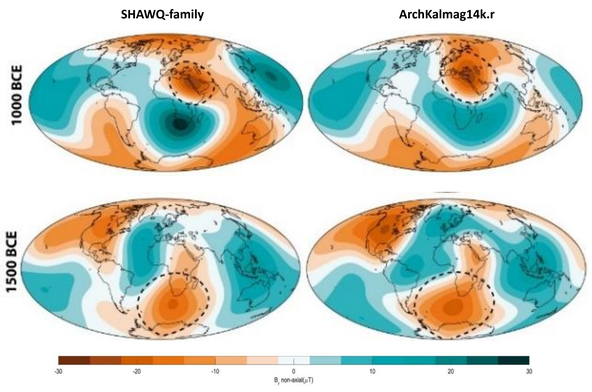


*Figure 1. Snapshots of the non-axial radial field $B_r^{non-axial}$ using the SHAWQ-family and ArchKalmag14k.r paleo-reconstructions. The dashed black circles show the regions where the studied non-axial field are located.*

We use the most recent archaeomagnetic models for the Holocene:

- SHAWQ-family (Campuzano et al., 2019; Osete et al., 2020)
- ArchKalmag14k.r (Schanner et al., 2022)

We identify these anomalies in the non-axial radial field: South Atlantic Non-Axial Anomaly **(SANAA)** and Levantine Iron Age Non-Axial Anomaly **(LIANAA)**

## 2- METHODS: Monopole model

We model the non-axial field anomalies in surface with a monopolar source at certain depth, using the radial component:

$$B_r^{non-axial} = B_r - B_r^{axial} = B_r^{anomaly}$$

The radial field of a monopole at Earth's surface is given by:

$$B_r^{monopole} = \mp \frac{\boldsymbol{k}\,[a - \boldsymbol{r_0}(sin\theta\, sin\boldsymbol{\theta_0}\cos(\varphi - \varphi_0) + cos\theta\, cos\boldsymbol{\theta_0})]}{[a^2 + \boldsymbol{r_0^2} - 2a\boldsymbol{r_0}(sin\theta\, sin\theta_0\cos(\varphi - \boldsymbol{\varphi_0}) + cos\theta\, cos\boldsymbol{\theta_0})]^{3/2}}$$

Monopole parameters:

- $\boldsymbol{k}$: strength
- $\boldsymbol{r_0}$: radius from Earth's center.
- $\boldsymbol{\theta_0}$, $\boldsymbol{\varphi_0}$: colatitude and longitude.

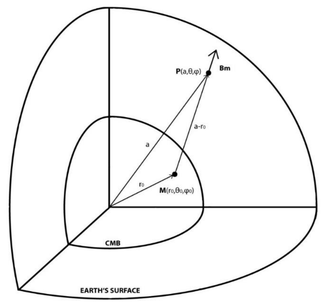


*Figure 2 . Sketch of the field created in surface by a positive monopole located in certain colatitude $\theta_0$, longitude $\varphi_0$ and distance $r_0$ to the Earth's center.*

## 3- Dependence with the grid size

The sensitivity of the monopole parameters with the grid size has been tested using two different circular regions centered in the maximum of the anomaly:

1- *Variable grid*: constant size ranging between a minimal and maximal value.
2- *Adaptive grid*: time-changing grid size that adapts to the size of the anomaly.

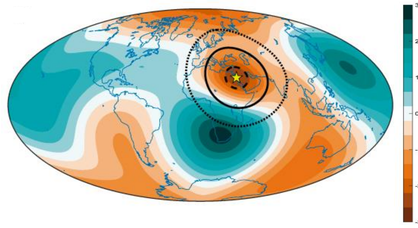


*Figure 3. $B_r^{non-axial}$ in Earth's surface for 1000 BCE for SHAWQ-family. In dots line the maximum grid size for LIANAA (45°); in dashed line the minimum grid size (10°); in thick line the adaptive grid size .*

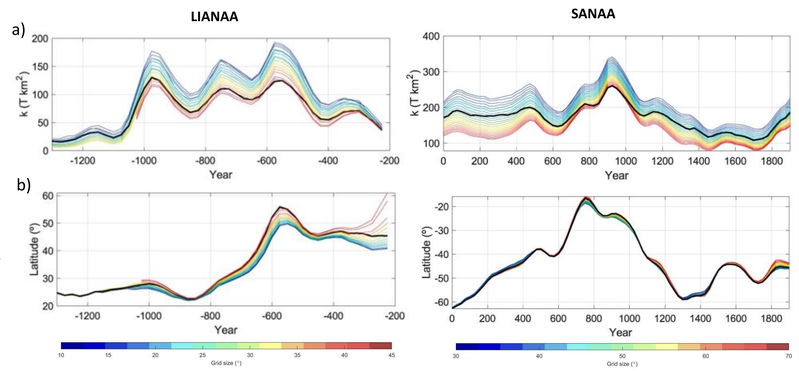


*Figure 4. Monopole parameters k (a) and latitude (b) for LIANAA (left) and SANAA (right) depending on the grid size. In colors the Variable grid ranging between 10° and 45° for LIANAA and between 30° and 70° for SANAA. In black dark line the monopole results for the adaptive grid size..*

## 4- RESULTS

### 4.1- Monopole model for Holocene anomalies

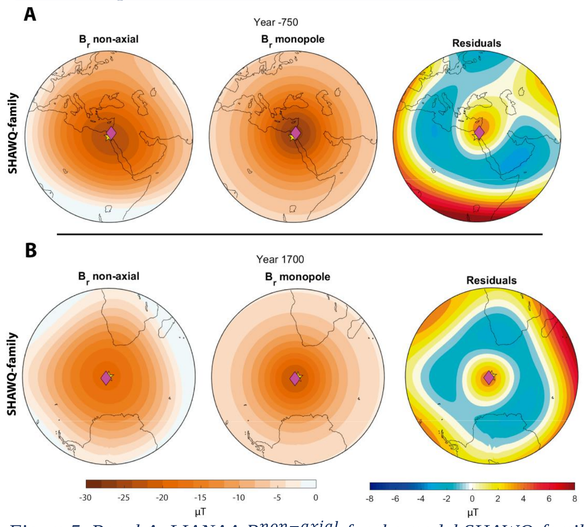


*Figure 5. Panel A. LIANAA $B_r^{non-axial}$ for the model SHAWQ-family in 750 BCE (left) , $B_r^{monopole}$ in Earth's surface (middle) and residuals $B_r^{non-axial} - B_r^{monopole}$ (right). The yellow star shows the location of the maximal anomalous field and the pink diamond shows the monopole location. Panel B for SANAA (1700 CE).*

### 4.2- Evolution of monopole parameters

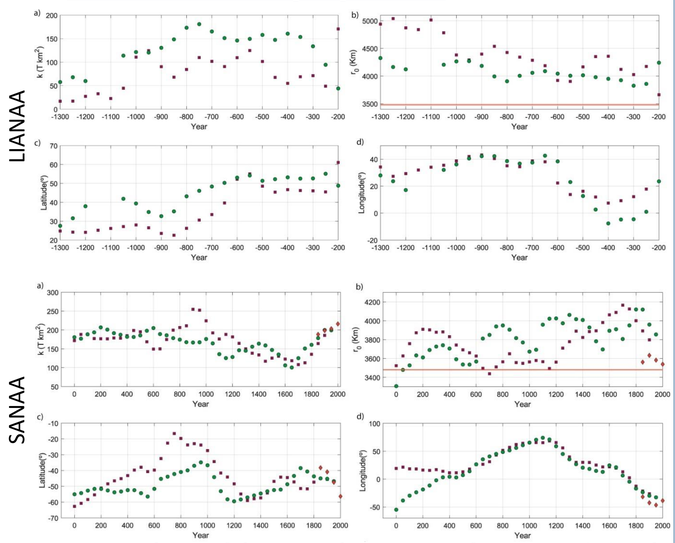


*Figure 6. Evolution of the monopole parameters for LIANAA (up) and SANAA (down) using the SHAWQ-family (red squares) and ArchKalmag.14k.r (green dots). For SANAA also the monopole model using the instrumental model COV-OBS.x2 (Huder et al., 2020) in orange diamonds from 1840 CE. The red horizontal line show the CMB radius.*

## 5- DISCUSSION: Relationship with LLSVPs

Some important geomagnetic features observed at the Earth's surface might be related to heterogeneous structure of the lower mantle.

The location of the monopoles for LIANAA and SANAA seems to follow the edges of the the African Large Low Shear Velocity Province (LLSVP).

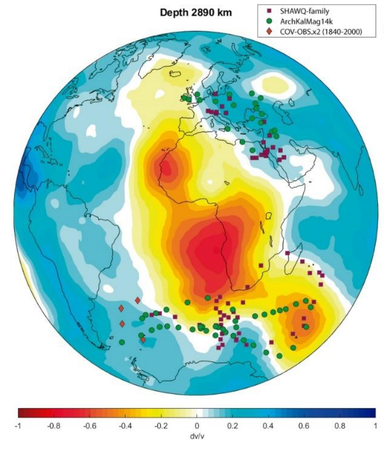


*Figure 7. Trajectories of the monopole for the SANAA and LIANAA for the different models used in this study, every 50 yr. In the colormap we represent the normalized S-velocity in the CMB, at 2890 km depth. The negative velocity anomaly values (yellow-red colors) characterize the African LLSVP.*

## 6- Conclusions

- The non-axial field show features of the field masked by the axial dipole. Models show the presence of a South Atlantic non-axial anomaly during the first millennium CE previous to SAA.
- The monopole model can be useful to characterize the evolution of circular-shaped anomalies as LIANAA and SANAA.
- Position of the monopoles linked with SANAA and LIANAA seem to match the edges of low s-velocity regions of the lower mantle. The link of anomalies to lower mantle heterogeneities suggest they might be recurrent or persistent features of the geomagnetic field.

## References

Campuzano SA, Gomez-Paccard M, Pavon-Carrasco FJ, Osete ML (2019) Emergence and evolution of the South Atlantic Anomaly revealed by the new paleomagnetic reconstruction SHAWQ2k. Earth Planet Sci Lett 512:17–26.

Huder, L., Gillet, N., Finlay, C.C. et al. (2020). COV-OBS.x2: 180 years of geomagnetic field evolution from ground-based and satellite observations. Earth Planets Space 72, 160.

Osete ML, Molina-Cardin A, Campuzano SA, Aguilella-Arzo G, Barrachina-Ibanez A, Fallomir-Granell F, Olver Foix A, Gomez-Paccard M, Martin-Hernandez F, Palencia-Ortas A, Pavon-Carrasco FJ, Rivero-Montero M. (2020) Two archaeomagnetic intensity maxima and rapid directional variation rates during the Early Iron Age observed at Iberian coordinates. Implications on the evolution of the Levantine Iron Age Anomaly. Earth Planet Sci Lett 533:116047.

Schanner, M., Korte, M., & Holschneider, M. (2022). ArchKalmag14k: A Kalman-Filter based global geomagnetic model for the holocene. Journal of Geophysical Research: Solid Earth, 127(2), e2021JB023166.

## Acknowledgements

The authors are grateful to the Spanish Ministry of Science and Innovation for supporting this research through the project PULSES.5K (PID2020-117105RB-I00), SUMATE (PID2020-113316GB-100) and CSIC i-LINK-22057. P.R. thanks the Spanish Ministry of Universities (FPU18/01567) for the funding of his PhD.